

## LITERATURE CITED

1. V. D. Gorshkov, A. N. Opanasenko, and N. N. Shan'gin, "Transient heat and mass exchange processes in elements of a nuclear reactor with an integral layout," in: Thermophysical Investigations [in Russian], Vol. 3, VIMI, Moscow (1977), pp. 34-40.
2. J. J. Lorenz and R. D. Carlson, "LMFBR outlet plenum flow stratification studies," Trans. Am. Nucl. Soc., 21, 418-419 (1975).
3. T. V. Kuskova, "Numerical study of two-dimensional flows of a viscous incompressible liquid," in: Certain Applications of the Grid Method in Gas Dynamics [in Russian], Vol. 3, Moscow State Univ. (1971), pp. 7-136.
4. M. K. Gorchakov, V. M. Kashcheev, A. N. Kolmakov, and Yu. S. Yur'ev, "Application of a model of a porous body to thermohydraulic calculations for reactors and heat exchangers," Teplofiz. Vys. Temp., 14, No. 4, 866-871 (1976).
5. E. V. Nomofilov and T. V. Romanova, "Investigation of certain features of liquid flow in rectangular and cylindrical distributing manifolds," Preprint FÉI-647 (1975).
6. V. I. Polezhaev and Yu. V. Val'tsiferov, "Numerical study of transient thermal convection in a cylindrical vessel with lateral heat inlet," in: Certain Applications of the Grid Method in Gas Dynamics [in Russian], Vol. 3, Moscow State Univ. (1971), pp. 137-174.
7. A. A. Samarskii and A. V. Gulin, Stability of Difference Schemes [in Russian], Nauka, Moscow (1973).

## STRUCTURE OF FLOWS IN VORTICES

V. A. Bubnov, I. Z. Gabdullin,  
and A. A. Solov'ev

UDC 532.517.4

The structure of a gradient vortical flow was studied experimentally.

Stationary vortex tubes, characterized by substantial radial changes in velocity, were excited by a vortex generator [1]. The frequency of rotation of the swirler was measured with a tachometer. Velocity and pressure were measured with a five-channel spherical probe which was moved radially and vertically.

Vortex generators are usually characterized by dimensionless parameters [2]. The values of certain of these parameters for the above generator are given in Table 1. Also shown here for the sake of comparison are values for the units in [3].

According to the data in [2], free vortices have sharp velocity gradients at the boundary of the core in those cases where the effective exchange coefficient  $s$  and ratio  $a^*/a$  are close to unity. The vortex generator we used did not allow us to independently change the velocity of the ascending flow or the angular momentum of the vortex. The parameter  $s$  thus changed within very narrow limits, whereas the generators in [3], with constant equipment dimensions, allowed for variation of this parameter. As concerns the parameter  $a^*/a$ ,

TABLE 1. Dimensionless Parameters Characterizing the Vortices

Parameter	Model		Parameter	Model	
	data from [3]	our data		data from [3]	our data
$\Gamma_\infty, \text{m}^2/\text{sec}$	1	1,3	$a^*$	1,6	2,0
$\text{Re}, 10^4$	5	8,5	$a^*/a$	0,11	0,9
$N, 10^4$	7,7	5,1	$s$	0,3	0,8
$a$	15	2,3	$s^*$	5,5	2,0

Moscow Machine-Tool Construction Institute. M. V. Lomonosov Moscow State University. Translated from Inzhenerno-Fizicheskii Zhurnal, Vol. 39, No. 4, pp. 611-618, October, 1980. Original article submitted June 11, 1979.

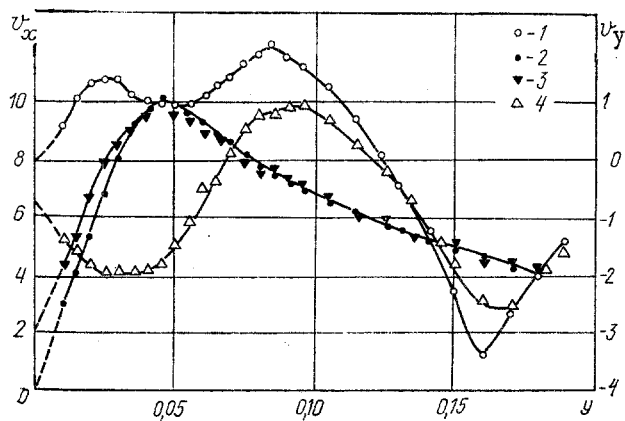


Fig. 1. Comparison of measurements of velocities in a vortex (m/sec): 1)  $v_\varphi$ ; 2)  $v_r$ , measured along a radius of the vortex; 3)  $v_x$ ; 4)  $v_y$ , measured along a chord.

which characterizes the ratio of the dimensions of the zone where the rotation is assigned to the length of the zone of ascending eddy currents, our generator has a distinct advantage over the generators in [3]. This is shown by the values of  $\alpha^*/a$  given in Table 1 and in the survey [2].

The above method of reproducing sufficiently stable gradient vortices under laboratory conditions opens up the possibility of experimentally investigating vortices with physical properties close to those actually encountered in nature.

To simultaneously measure the pressure and velocity vector, we used a five-channel spherical probe with a ball 0.003 m in diameter and a holder rod 0.0018 m in diameter. The measurement method amounted to determining the angle  $\vartheta$  of the orientation of the central hole in the probe relative to the flow and measuring pressure in the corresponding holes by means of a Prandtl macromanometer.

The macromanometer scale was graduated in divisions of 0.1. The error in determining the difference in the pressures between the outermost holes in the probe ball averaged 1%. Taking into account the error in calculating the angle of taper  $\delta$  in the plane of the meridian according to probe calibration curves, the average error of the velocity modulus measurement did not exceed 1-2%. The actual error is larger and is associated mainly with errors that arise as a result of the gradient character of the flows [4].

According to the measurements made at an elevation of 0.015 m, the difference in the readings of the manometers attached to the outermost holes of the probe falls from a value of 18 divisions at the boundary of the vortex core (at  $r=0.05$  m) to zero on the axis of the vortex (at  $r=0$ ). Consequently, the manometer readings change by 0.36 divisions over

TABLE 2. Relative Error of Measurements of Tangential Velocity in a Series of Three Tests

r, m	Tangential velocity $v_\varphi$ , m/sec				$\frac{\Delta v_\varphi}{v_\varphi}$ , %
	test 1	2	3	mean	
0,21	2,9	3,6	2,4	3,0	1,2
0,18	3,9	4,3	4,3	4,2	4,0
0,15	4,5	4,8	4,8	4,7	2,8
0,13	5,6	5,8	5,6	5,7	1,8
0,12	6,0	6,0	5,9	6,0	0,6
0,106	6,8	7,0	6,8	6,9	1,5
0,08	8,1	7,9	8,0	8,0	1,3
0,06	8,7	8,7	8,8	8,7	0,4
0,045	10	9,7	9,7	9,8	1,4
0,035	8,8	8,9	9,4	9,0	2,6
0,030	7,1	7,3	8,1	7,7	6,0
0,020	6,2	5,9	5,4	5,8	5,2
0,005	3,5	2,3	2,4	2,7	18,5

TABLE 3. Experimental Data on Tangential Velocity in a Vortex Tube

r, cm	Distance from subjacent surface, m									
	0,015	0,029	0,043	0,058	0,068	0,075	0,090	0,103	0,118	0,134
1,0	2,1	2,0	2,1	2,1	2,0	2,1	2,1	2,1	2,1	2,1
2,0	4,2	4,1	4,3	4,1	4,1	4,2	4,1	4,2	4,1	4,3
3,0	6,3	6,2	6,1	6,3	6,2	6,2	6,1	6,3	6,1	6,2
4,0	8,3	8,0	7,7	7,5	7,4	7,4	7,3	7,3	7,2	7,1
5,0	9,5	8,8	8,4	8,1	8,0	7,8	7,6	7,5	7,4	7,3
6,0	8,9	8,4	8,1	7,8	7,7	7,5	7,2	7,1	7,0	6,9
7,0	8,2	7,9	7,5	7,3	7,2	6,9	6,7	6,5	6,5	6,2
7,5	7,8	7,6	7,3	7,0	6,9	6,7	6,4	6,3	6,2	5,9
8,0	7,4	7,2	7,1	6,8	6,7	6,5	6,2	6,1	6,0	6,4
8,5	7,0	6,9	6,9	6,6	6,5	6,3	6,2	6,2	6,2	7,4
9,0	6,6	6,4	6,8	6,5	6,7	6,6	6,6	6,8	7,1	8,6
10,0	6,1	5,9	6,7	7,0	7,2	7,6	7,8	8,5	9,2	11
10,5	5,9	6,1	6,8	7,3	7,6	8,0	8,5	9,3	10,3	11,8
11,0	5,7	6,1	6,9	7,5	7,9	8,4	9,2	9,9	10,8	12,1
11,5	5,6	6,2	7,0	7,7	8,1	8,5	9,5	9,8	10,2	11,3
12,0	5,5	6,2	7,1	7,6	8,1	8,4	9,2	9,0	8,8	8,5
12,5	5,4	6,2	6,9	7,2	7,6	7,9	8,3	8,0	7,0	4,1
13,0	5,3	6,0	6,5	6,6	7,0	7,3	7,0	6,7	5,5	2,2
14,0	4,8	4,7	4,9	5,4	5,5	5,2	4,7	4,0	2,9	1,7
15,0	4,3	4,3	4,1	3,7	3,8	3,7	3,4	3,0	2,1	1,5
16,0	3,8	3,5	3,2	2,8	2,6	2,1	1,6	1,2	1,1	1,2
17,0	3,4	3,2	2,7	2,3	1,8	1,4	0,9	0,7	0,8	1,1
18,0	3,0	2,8	2,3	1,6	1,4	0,7	0,5	0,4	0,7	1,0
19,0	2,6	2,5	2,0	1,1	1,0	0,4	0,4	0,3	0,7	0,9

a distance of 0.001 m between the outermost holes in the probe. This value amounts to 2% of the maximum difference in pressures in the zone of large velocity gradients. On the whole, the relative error of the measurements of the velocity modulus is 3.3%, taking into account the velocity gradient.

The velocity components were computed from the following formulas:

$$v_x = v \cos \delta \sin \vartheta; v_y = v \sin \delta; v_z = -v \cos \delta \cos \vartheta. \quad (1)$$

The origin of the rectangular system of probe coordinates (x, y, z) was located in the center of the ball. The y axis was directed along the axis of the holder, while the z axis was perpendicular to the plane of the investigated cross section (x, y) and was directed upward. Since the angles  $\vartheta$  were reckoned from the positive direction along the z axis, the last formula in (1) has a minus sign (in contrast to the similar formula in [5]).

On the average in the measurements, the angle  $\delta \approx 15^\circ$ , while  $\vartheta \approx 100^\circ$ . The absolute error in the determination of  $\vartheta$  and  $\delta$  was equal to 0.5 and 0.1°, respectively. The errors in the determination of the velocity components: 4% for  $v_x$ ; 6.5% for  $v_z$ ; 10.5% for  $v_y$ . The error of static pressure was 4%.

These should be regarded as the maximum errors. Table 2 shows the results of experiments conducted under the same conditions. The errors are no greater than 4% for most of the vortex, as can be seen from the data. However, these errors increase substantially on the vortex axis. The mean error for the entire range of measurements through the vortex radius was 2.4%, except for the values at  $r = 0.005$  m.

Substantial errors may arise in those cases where the measurement direction does not coincide with a radius of the vortex. This question is practically ignored in the literature on velocity measurements obtained with total pressure transducers. Our estimates show that when the probe is moved along a chord rather than a radius of the vortex, the velocity components calculated from Eqs. (1) will deviate significantly from the velocity projections on the axes of a cylindrical coordinate system connected with the center of the vortex.

Let a left-handed coordinate system have its origin at the center of a vortex tube on a subjacent surface. The following formulas are used to change over from  $v_x$ ,  $v_y$ , and  $v_z$  in the rectangular coordinate system (x, y, z) to the velocity components  $v_\varphi$ ,  $v_r$ , and  $v_z$  in a cylindrical system of vortex coordinates:

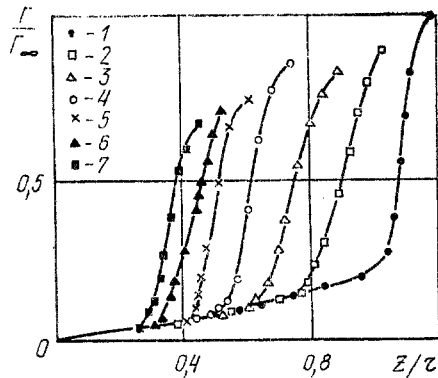


Fig. 2

Fig. 2. Evaluation of similitude of the flow at different distances from the lower ring of the vortex (m): 1) 0.134; 2) 0.118; 3) 0.103; 4) 0.09; 5) 0.075; 6) 0.068; 7) 0.058.

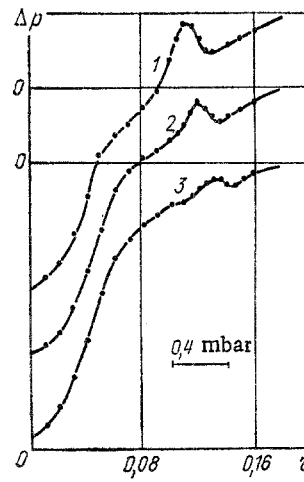


Fig. 3

Fig. 3. Radial profiles of pressure  $\Delta p$ , mbar, at different elevations  $z$ , m: 1)  $z = 0.134$ ; 2) 0.90; 3) 0.29.

$$v_\varphi = -v_x \sin \varphi + v_y \cos \varphi, \quad v_r = v_x \cos \varphi + v_y \sin \varphi, \quad v'_z = v_z. \quad (2)$$

It is apparent from (2) that the following holds only in the case when the probe measurements are made in radial directions in the vortex, i.e.,  $\varphi = 90^\circ$

$$v_\varphi = -v_x; \quad v_r = v_y; \quad v'_z = v_z. \quad (3)$$

Velocity may be measured along directions other than radial as a result of inaccurate or erroneous determination of the center of the vortex. Figure 1 shows measurements of the velocity components along two parallel directions in the first quadrant for a coordinate system connected with a vortex. One of the directions was along a radius of the vortex, so that Eqs. (3) could be used for this direction. The other direction was along a chord located 0.013 m from the nearest radius. It is apparent from Fig. 1 that the probe measurements of  $v_x$  and  $v_y$  deviate from the experimental data in the previous case. If the measurements obtained along the chord are interpreted in the same manner as those obtained along a radius, i.e. if Eqs. (3) are used, then — as can be seen from comparing the graphs — we permit an error which lies far outside the limit of the theoretical accuracy of the method.

The above discussion shows the need to accurately determine the center of the vortex. The geometrical center of the chamber is usually taken as the center of the vortex in studying vortices in chambers and tubes. However, this method is unsuitable in our case, where the vortex is not confined by lateral walls. The fact that the velocity component  $v_z$  in both coordinate systems was computed by the same formula was used to determine the position of the vortex center. For this purpose, we measured  $v_z(x)$  at an assigned height, with a fixed value of  $y$ . The distance between  $x_1$  and  $x_2$ , where  $v_z = 0$ , represents a chord. A perpendicular was drawn through the center of this chord. Obviously, this perpendicular is directed along a radius of the vortex. The value of the radius on which the tangential velocity  $v_\varphi = 0$  and changes sign corresponds to the center of the vortex.

Vortex tubes with a steep velocity gradient in the zone of the transition from solid revolution to potential flow were experimentally studied in [6]. However, in this investigation the measurements were only qualitative in character.

In all of the tests we conducted, the gradient vortex tubes were excited under conditions of an angular swirler velocity of 2400 rpm. The length of the vortex tube from the subjacent surface to the swirler blades was 0.215 m. Three independent measurements were made in most cases.

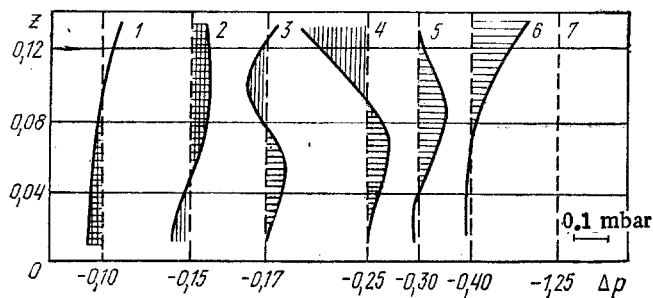


Fig. 4. Measurement of static pressure along the vertical at different distances from the vortex axis ( $r$ , m): 1)  $r = 0.015$ ; 2) 0.13; 3) 0.12; 4) 0.11; 5) 0.10; 6) 0.097; 7) 0.04.

It turned out that a fairly broad zone existed between the region of solid revolution and potential flow. In this zone, the tangential component of velocity passes through a minimum, and a steep gradient is seen after the second maximum. Such a character of change in the tangential velocity along the vortex radius is different from the velocity profiles usually seen.

Table 3 shows values of tangential velocity obtained by measurement at ten elevations from the subjacent surface. It should be pointed out that the intensity of the second maximum decreases with increasing distance from the swirler. In the measurements close to the subjacent surface, the intensity of the second maximum is negligible compared to that of the first maximum and may go unrecorded in the case of relatively coarse measurements.

Since the Navier-Stokes equation makes it possible to obtain similitudinous solutions for vortical flows, the question arises as to checking the similar character of the flow in the present case.

It is apparent from Fig. 2 that the tangential velocity component, with the coordinate  $z/r$ , is not in similitude for all values of  $r$ . The minimum value of  $r$  at which flow regime similitude is first seen increases with a decrease in  $z$ . If these minimum values of  $r$  are matched with the values of  $z$  at which the measurements were made, we obtain a line which is approximated well by the equation

$$z = -0.77r + 0.238, \quad (4)$$

with  $r$  and  $z$  being measured in meters.

All points on the  $(z, r)$  plane lying to the right of this straight line define the region of flow similitude with respect to the coordinate  $z/r$ . The Reynolds number in these tests was  $8.5 \cdot 10^4$ . The results obtained show that the similitude of the flow for the present case is of a limited nature.

We also observed the existence of an annular zone of high static pressure beyond the boundary of solid revolution in the vortex model we investigated (Fig. 3). The pressure profiles we obtained differed from the curves usually seen, such as in [3]. Pressure curves with bump on their periphery were noted earlier [7] in natural vortices and under laboratory conditions. The local increase in pressure is evidently connected with the large transverse gradients of the radial velocity component. Away from the swirler, tangential flow begins to predominate over radial flow, and the peaks on the profile are smoothed out. This result follows from the measurements of pressure at different elevations and on different radii shown in Fig. 3.

The unusual character of the static pressure profiles beyond the boundary of solid revolution can also be followed on curves of the change in pressure with elevation. It is apparent from Fig. 4 that the change in pressure along vertical directions is of an oscillatory nature. The pressure and profiles of axial velocity (Table 4) are the same at all elevations in the core zone of the vortex. Consequently, two-dimensional vortical flow occurs in this zone, which confirms the Taylor-Proudman theory [8].

TABLE 4. Results of Measurements of Axial Velocity Component over the Height and Radius of the Vortex,  $v_z(r, z)$ , m/sec

$r, m$	Distance from subjacent surface, m									
	0,015	0,029	0,043	0,058	0,068	0,075	0,09	0,103	0,118	0,134
0,010	0,6	0,6	0,6	0,6	0,6	0,6	0,6	0,6	0,6	0,6
0,020	1,4	1,4	1,4	1,4	1,4	1,4	1,4	1,4	1,4	1,4
0,030	2,3	2,3	2,3	2,3	2,4	2,3	2,4	2,4	2,3	2,3
0,035	2,9	2,9	3,0	2,9	3,0	3,0	2,9	2,9	2,9	2,9
0,040	3,3	3,5	3,5	3,4	3,4	3,5	3,5	3,5	3,4	3,5
0,045	3,4	4,0	4,0	3,9	3,9	4,0	3,9	3,9	4,0	4,0
0,050	3,5	4,2	4,4	4,5	4,5	4,5	4,5	4,5	4,5	4,5
0,055	3,3	4,0	4,4	4,6	4,6	4,6	4,6	4,6	4,6	4,6
0,060	3,0	3,6	4,2	4,5	4,5	4,5	4,5	4,5	4,5	4,5
0,065	2,6	3,2	3,9	4,2	4,2	4,1	4,1	4,2	4,1	4,1
0,070	2,2	2,8	3,5	3,9	3,8	3,9	3,8	3,8	3,9	3,9
0,075	1,9	2,4	3,0	3,5	3,5	3,4	3,5	3,5	3,4	3,5
0,080	1,5	2,0	2,5	2,9	2,9	3,0	2,9	3,0	3,0	3,0
0,090	0,8	1,1	1,5	1,9	1,9	1,8	1,9	1,9	1,9	1,9
0,100	0	0	0	0	0	0	0	0	0	0
0,105	-0,2	-0,3	-0,4	-0,5	-1,0	-1,5	-2,4	-3,2	-3,8	-4,3
0,110	-0,5	-0,7	-0,9	-1,1	-1,9	-2,2	-3,2	-4,0	-4,7	-5,1
0,115	-0,7	-1,1	-1,3	-1,8	-2,8	-3,4	-4,2	-4,6	-5,0	-4,3
0,120	-0,9	-1,5	-1,8	-2,5	-3,7	-4,2	-4,7	-4,8	-4,3	-2,0
0,125	-1,0	-1,8	-2,2	-3,0	-4,2	-4,5	-4,7	-4,2	-3,0	-0,3
0,130	-1,0	-2,0	-2,5	-3,1	-4,3	-4,6	-4,2	-3,4	-2,0	+0,1
0,135	-1,1	-2,0	-2,6	-3,1	-4,1	-4,3	-3,5	-2,4	-0,8	+0,4
0,140	-1,1	-1,9	-2,3	-2,8	-3,7	-3,7	-2,8	-1,7	0	0,5
0,145	-0,9	-1,7	-2,0	-2,4	-3,0	-2,8	-2,0	-1,0	0,2	+0,6
0,150	-0,8	-1,4	-1,7	-2,0	-2,2	-2,0	-1,3	-0,4	0,3	0,6
0,155	-0,7	-1,1	-1,4	-1,6	-1,18	-1,4	-0,7	0	0,4	0,7
0,160	-0,5	-0,9	-1,2	-1,3	-1,3	-0,9	-0,3	0,1	0,5	0,7
0,170	-0,3	-0,5	-0,7	-0,6	-0,5	-0,2	0,2	0,5	0,6	0,7
0,190	-0,1	-0,1	0	0,1	0,3	0,4	0,5	0,6	0,6	0,6

Pressure varies with height outside the zone of solid revolution. Local deviations are established relative to fixed pressure values. These deviations, originating close to the swirler, are displaced downwards toward the subjacent surface with an increase in the distance from the boundary of solid revolution (see the hatched sections of the curves  $\Delta p(z)$  at different values of  $r$  in Fig. 4). The oscillatory character of the vertical profiles suggests waves, excited by the swirler and maintained by rotation [7]. Whereas, within the framework of linear theory, the velocity of the secondary flows ( $v_z, v_r$ ) is an order lower than the velocity of the main flow  $v_\varphi$  in normal flows, in gradient flows these velocities and their gradients become comparable — a fact which evidently leads to the new phenomena noted above.

#### NOTATION

$v_x, v_y, v_z$ , flow velocity components in a rectangular coordinate system;  $v_\varphi, v_r, v_z$ , flow velocity components in a cylindrical coordinate system;  $v_1$ , tangential velocity at the boundary of solid revolution at  $r=r_1$ ;  $l$ , length of the vortex;  $\nu$ , kinematic viscosity;  $R$ , radius of the forming cylinder;  $\Gamma_\infty$ , circulation in the region of potential flow;  $Q = 2\pi \int_0^{r_0} v_z r dr$ , second air flow rate through the eddy of ascending flows,  $0 \leq r \leq r_0$ ;  $Re = v_1 r_1 / \nu$ , tangential Reynolds number;  $N = Q / r_0 \nu$ , radial Reynolds number;  $a = l / r_0$ , configuration ratio for the vortex model;  $s = r_0 \Gamma_\infty / 2Q$ , effective exchange coefficient;  $a^* = l / R$ , configuration ratio for the vortex generator;  $s^* = R \Gamma_\infty / Q$ , constructive exchange coefficient;  $\Delta p = p - p_\infty$ , pressure drop in the vortex relative to atmospheric pressure  $p_\infty$ ;  $r^* = r / r_1$ , dimensionless radius of the vortex;  $v^* = v_\varphi / v_1$ , dimensionless tangential velocity;  $a^*/a$ , gradient ratio.

#### LITERATURE CITED

1. O. G. Martynenko, V. A. Bubnov, and A. A. Solov'ev, "Experimental investigations of vortex tubes," in: Processes of Heat and Mass Exchange in Elements of Thermo-optical Instruments [in Russian], ITMO im. A. V. Lykova Akad. Nauk BSSR, Minsk (1979), pp. 79-109.
2. R. P. Davies-Jones, "Laboratory simulation of tornadoes," Proc. of Symposium on Tornadoes, Texas Technol. Univ., Lubbock, Texas (1976), p. 151.

3. C. A. Wan and C. C. Chang, "Measurement of the velocity field in a simulated tornado-like vortex using a three-dimensional velocity probe," *J. Atmos. Sci.*, 29, 116-126 (1972).
4. I. I. Smul'skii, "On features of velocity and pressure change in a vortex chamber," in: *Thermophysics and Physical Hydrodynamics*, Institute of Thermophysics, Novosibirsk (1978), pp. 125-132.
5. I. L. Povkh, *Aerodynamic Experiments in Machine Design* [in Russian], Mashinostroenie, Leningrad (1974).
6. N. P. Kasterin, A. K. Timiryazev, and T. M. Sviridov, "Experimental production of a vortical air column," *Vestn. Mosk. Univ., Fiz.*, No. 10, 53-58 (1949).
7. N. B. Ward, "The exploration of certain features of tornado dynamics using a laboratory model," *J. Atmos. Sci.*, 29, 1194-1204 (1972).
8. H. R. Greenspan, *Theory of Rotating Liquids* [Russian translation], Gidrometeoizdat, Leningrad (1975).

RADIATION OF INTERNAL WAVES DURING VERTICAL MOTION  
OF A BODY THROUGH A NONUNIFORM LIQUID

V. A. Gorodtsov

UDC 532.58

Energy losses to radiation of internal waves during the vertical motion of a point dipole in two-dimensional and three-dimensional cases are computed.

During the motion of bodies in a liquid with nonuniform density in the field of gravity, in addition to sound waves, internal gravitational waves are also excited in the liquid, and the body due to the loss of wave momentum experiences an additional wave resistance. A simpler problem concerning the motion of singular sources, in some sense approximately equivalent to the bodies, is often examined within the framework of the linear description of the wave field [1-4]. Such substitutions are well known and have a precise meaning in the theory of a uniform ideal liquid. It is assumed that they can also be used in the case of a weakly nonuniform liquid. In what follows, within the framework of a similar approach, we compute the total energy losses due to the formation of waves during vertical motion of bodies with subsonic speeds.

Neglecting dissipation processes in the liquid, its motion as excited by a source with mass  $\rho m$  can be described with the help of the equations describing the balance of forces and mass and the condition of adiabaticity. If in the absence of the source, the liquid is stationary and the pressure  $p_0(z)$  and density  $\rho_0(z)$  depend only on the vertical coordinate  $z$ , then for small perturbations the basic equations can be written in the following linearized form [5, 6]:

$$\begin{aligned} \rho_0 \hat{D}\mathbf{v} + \nabla p &= \rho \mathbf{g}, \quad \hat{D}\rho + \rho_0 \omega H^{-1} + \rho_0 \nabla \mathbf{v} = \rho_0 m, \\ \hat{D}p + \rho_0 \omega g &= c_0^2 (\hat{D}\rho + \rho_0 \omega H^{-1}), \quad H^{-1} \equiv \frac{d \ln \rho_0}{dz}, \end{aligned} \quad (1)$$

where  $\hat{D}$  denotes the operator for differentiation with respect to time.

From this system of equations, it is easy to obtain separate equations for perturbations of pressure, density, and velocity. The pressure equation in the case of a liquid with constant coefficients  $H$  and  $N^2 \equiv gH^{-1} - g^2 c_0^{-2}$  can be put into the form

$$\hat{L}p^0 = - \left( \frac{\partial^2}{\partial t^2} + N^2 \right) \frac{\partial}{\partial t} m^0,$$

---

Institute of Problems in Mechanics, Academy of Sciences of the USSR, Moscow. Translated from *Inzhenerno-Fizicheskii Zhurnal*, Vol. 39, No. 4, pp. 619-623, October, 1980. Original article submitted August 10, 1979.